Composite Structures 140 (2016) 668–674

Contents lists available at ScienceDirect

Composite Structures

journal homepage: www.elsevier.com/locate/compstruct

Simulating the warping of thin coated Si wafers using Ansys layered shell elements

J. Schicker *, W.A. Khan, T. Arnold, C. Hirschl

CTR Carinthian Tech Research AG, Europastraße 12, 9524 Villach, Austria

ARTICLE INFO

Article history:
Available online 6 January 2016

Keywords:
Thin-film-on-substrates
Anisotropic material
FEM
Ansys layered shell elements
Large deflections
Stoney's formula

ABSTRACT

The feasibility of simulating thin-film-on-substrates behaviour of large thin coated wafers using Ansys® "layered shells" is estimated. Layered shell elements are based on Mindlin-plates with coupled intrinsic layers. These elements can be used with an update Lagrange algorithm (NLGEOM). They are of interest because they are easy to use and require a minimum of degrees of freedom to discretize a coated wafer. More traditional discretisations with two separate element layers are used for evaluating the Finite Element (FE) solution.

The simulation results are further compared to results reported in the literature and to the analytical approach of Stoney (1909). For this purpose, a thorough review of the Stoney approach is done. We present an extended version with a plate stiffness for cubic anisotropic material and an additional formula to calculate the curvature from the thermal strain mismatch. It is shown that Stoney's approach to estimate the film stress from the curvature is inadequate for large deflections. A direct comparison to bending experiments with large thin coated wafers cannot be given since the deflection of these wafers is interfered from a predominant deflection from their dead load.

1. Introduction

When wafers[1] are thick with small diameters, i.e. $t > 500$ μm and $2R \leqslant 200$ mm, handling during the fabrication process is not difficult and simple linear estimates are sufficient for the description of the wafers mechanical behaviour. The current trend is to produce larger and thinner wafers. Clearly, these require more care during processing and the description of their mechanical behaviour becomes more complex.

Actual wafer sizes of 300 mm diameter are state of the art and manufacturers are on the verge of initiating a 450 mm diameter wafer. However, many applications require thinner wafers than can be obtained by sawing. These wafers are thinned by grinding. Wafer thicknesses of less than 200 μm until 60 μm are not unusual. Grinding induces intrinsic compressive stresses from texture disturbance in a subsurface layer of some 80 nm thickness [2,3]. These stresses reach high values. Chen and de Wolf [3] specify the compressive stresses from grinding as 100–150 MPa. Sun et al. [4] give values of 1 GPa and higher. It is possible to totally remove these stresses by etching [3]. The thinned wafers are then plated on one side with one or more thin metal layers of a few 100 nm. The metallic layers are baked at high temperature. When cooled to room temperature, most metals shrink differently from the silicon substrate due to their different thermal expansion coefficients. The stresses arising from the thermal mismatch can not be removed and, even in absence of other loads, the wafers are bent by eccentric in-plane forces. The warping shape depends, among other things, on the thickness ratios and the crystal orientations. In large thin wafers the out of plane deflection can exceed 10 times the wafer thickness. Thus, a linear model for the bending behaviour yields poor estimates and leads to false conclusions. This paper attempts to improve the estimate.

2. Review of the thin film on substrates problem

A coated plate with uniform in plane stress in the coating layer and a different stress in the substrate develops additional strains to balance the internal forces. If the coating is applied on only one side of the plate, the additional strains vary over the composite plate's thickness and induce plate bending. The first approach to calculate the stress mismatch from a measurement of curvature was presented by Stoney in 1909 [1]. There, a linear relationship was presented for a uniaxial strip with a significantly thinner

* Corresponding author. Tel.: +43 (0)4242 56300x217.
E-mail addresses: johannes.schicker@ctr.at (J. Schicker), thomas.arnold@ctr.at (T. Arnold), christina.hirschl@ctr.at (C. Hirschl).

[1] Mechanically, a wafer is a circular plate with a diameter to thickness ratio in the order of 100:1–1000:1. The coating is again three orders smaller than the thickness of the bare substrate. A wafer has a distinct crystal orientation.

http://dx.doi.org/10.1016/j.compstruct.2015.12.062
0263-8223/

coating. Later, this relation was extended to a biaxial form, still addressed as Stoney's formula. This relation is easy to implement and is frequently used, even in problems where a linear relation is obviously inappropriate. In this paper we consider the error that develops in these cases. If the misfit stress originates from thermal expansion of an originally planar plate, both the curvature and the film stress can be calculated for a given geometry and known material parameters if linear elasticity is assumed. The formulae are given in Appendix A.

Analytical examination of thin isotropic films on isotropic substrates with large deflections reveals a bifurcation point beyond which the spherically deformed shape may instantly turn into a more stable cylindrical shape [5–8]. Spherical warping is then still a possible solution but is unstable and a tiny moment suffices for abrupt turning into cylindrical shape, whereas the cylinder axis is arbitrary. In [9] an estimate is presented based on Finite Element (FE) simulations for a critical stress parameter $A_c = 680$ GPa for a circular silicon substrate. The stress parameter A is defined as

$$A = \sigma_f h_f \frac{D^2}{h_s^3} \tag{1}$$

with h_f the film thickness and h_s the substrate thickness, D is the plate diameter and σ_f the film stress. In [9] an explication is given: *the parameter A controls the extent of large deformations. For film stresses leading to A higher than the critical value, a cylindrical shape can be expected. For film stresses leading to A being lower than* $0.2A_c$ $(0.1A_c)$ *the linear Stoney approximations can be used with an error of less than* 10% (5%) *to a nonlinear FE solution. Between* $0.2A_c$ *and* A_c *a spherical shape is retained but the curvature and the film stress are in nonlinear relationship and the curvature varies across the wafer even when the film stress is uniform.*

Janssen et al. [10,11] extended Stoney's formula for cubic anisotropic substrates in a (001)-crystal plane and investigated the warping behaviour experimentally [10] for film stresses leading to $A < 0.2A_c$ on $D = 100$ mm wafers with $h_s \approx 500$ μm. They found that even at low film stresses the warping of anisotropic wafers is far more complicated than predicted by the isotropic model and that the curvature depends on the angle of the crystal lattice to the radial direction and varies with the location on the wafer.

2.1. Simulation approaches found in the literature

In contrast to the amount of theoretical and experimental investigations, few simulation approaches are reported in the literature. Common to all is the approach to induce the film stresses by thermal expansion.

Masters and Salamon made FE simulations for a rectangular plate using a combination of 20-node solid elements for the 127 μm thick substrate and 8-node shell elements for the 50 nm thick substrate with $L = 100$ mm edge length [7]. The simulations achieved the cylindrical shaped deflection only by applying a non-uniform film stress. The FE simulations gave a slightly higher film stress at bifurcation than was predicted theoretically.

Finot et al. [9] used 4-node shell elements for the substrate and 3 layers of shell elements for 3 stacked layers of different films for their predictions. The geometrical properties and the film stresses were varied. The wafer sizes ranged from D/h_s = 150/0.675 over 150/0.325 and 200/0.730 to 200/0.400 mm and the film thicknesses were between 0.9 and 2.4 μm. To convert the spherical warping to a cylindrical they applied a small moment.

3. Simulation approaches

In this paper we focus on calculation schemes to estimate the warping of large thin coated wafers by a stress mismatch from different thermal expansions of the coating film and the substrate. The derivation of the film material parameters from experiments, however, is not addressed here. Instead, we use an assumed film stress and assumed film properties. A direct comparison to experiments can not be given here because the real warping of large thin coated wafers must also consider an additional warping from dead load deformation. These wafers bulge strongly from their dead load, and, even with high film stresses, the warping from dead load seems to be predominant.

3.1. For calibrating the model

In the first task we compare FE results to an analytical estimate. Further, we evaluate the ability of "layered shells" to predict the out-of-plane deflection from the in-plane stress application with a result comparable to other discretisations. And we assess the benefit in effort. The reason for using "layered shells" is that it could be demonstrated earlier [12] that they are well suited for predicting bending problems of bare wafers with external loadings.

For this first simulation approach, a standard sized small wafer of 150 mm diameter and a thickness of 700 μm is considered. The coating has a thickness of 0.3 μm. For simplicity, we use constant thermal expansion coefficients with a difference from film to substrate of $\Delta\alpha^{\vartheta} = 5.4 \times 10^{-6}\ \mathrm{K}^{-1}$ and a temperature decrease of 580 °C. For the substrate we use two material assumptions: one of an isotropic approximation with a Young's modulus of $E = 160$ GPa and a Poisson's ration of $\nu = 0.22$, and one with a cubic anisotropic elastic Hooke's law with $c_{11} = 165.6$ GPa, $c_{12} = 63.9$ GPa, and $c_{33} = 79.5$ GPa according to [13]. For the film we use uniformly an isotropic linear elastic material with a supposed Young's modulus of $E = 210$ GPa and a Poisson's ratio of $\nu = 0.3$.

Using the extended Stoney formulae given in the appendix, a film stress of 935 MPa is obtained by Eqs. (A.20) and (A.26) for both substrate material models. This yields 0.027 times the critical film stress, σ_c^f, according to Eq. (1), i.e the film stress that results in $0.027 \times A_c$, and thus, Stoney's linear approximation should suffice for an analytical estimate. From Eq. (A.27) we finally obtain a deflection at the rim of the wafer of $w(R) = 0.0471$ mm for an isotropic substrate material and 0.0536 mm for an anisotropic.

To evaluate the possibilities for computing this problem using the Ansys® Mechanical Finite Element package (Versions 15, 2014, and 16, 2015) the problem is discretized using different types of elements. As a first model, similarily to the approach of Masters and Salamon [7], we use 20-node solids (brick elements) for the substrate and 8-node shell elements for the film. But in contrast to Masters and Salamon, we use a contact formulation for joining the two layers. The contact algorithm itself is varied. Further, we use 4-node and 8-node shell elements for substrate and film in our second model. A first subtype of this model uses a contact formulation for joining the layers and nodes located in the centre-planes of the respective shells. The second subtype uses common nodes at the layers interface. The shell elements then with an offset of the nodes from their centre planes. Finally, as third model we use one layer of "layered shell" elements. These are elements with the layer properties intrinsically embedded and using a Kirchhoff relation for the layer interaction inside the element, whereas the element itself is a standard Mindlin-plate shell with rotational and displacement degrees of freedom. It should be emphasised, that no averaging of the layer properties is done. In the Finite Element calculations, we use both a geometrical linear and a geometrical nonlinear approach to solve the problem.

3.2. For the application on large thin wafers

In the second task we use the FE analysis to estimate the warping behaviour of large thin coated wafers from thermally induced

mismatch stresses. We concentrate on using layered shell elements. The results of the FE solutions are again compared to the predictions by the Stoney approach and to results reported in literature.

Here, we consider a large thin wafer with a high film stress. The wafer geometry is much more slender with 300 mm diameter and 200 μm thickness. The thickness of the film is, as before, 0.3 μm. Also the mechanical properties are equal to those of the compact wafer of the first task. The final temperature decrease is higher with −780 °C. It is applied in 800 time steps and, hence, all stages of film stresses can be evaluated.

Using the Stoney equations in the appendix as a first estimate, the temperature drop can be calculated at which the critical film stress according to Eq. (1) is reached. With it, the critical film stress for this wafer accounts for $\sigma_c^f = 201$ MPa, and thus $0.2\,\sigma_c^f = 40$ MPa. This yields a theoretical temperature drop of 25 °C to obtain $0.2\,\sigma_c^f$ and 126 °C to obtain σ_c^f, i.e. 0.032 and 0.162 of the total applied load, respectively. The rim deflection at $0.2\,\sigma_c^f$ yields $w(R) = 0.0989$ mm for the isotropic and $w(R) = 0,11255$ mm for the cubic anisotropic wafer using these equations. Further, at σ_c^f the linear Stoney theory predicts a rim deflection of $w(R) = 0.4968$ mm for the wafer with isotropic and $w(R) = 0,5656$ mm for that with cubic anisotropic substrate behaviour. The full temperature drop of 780 °C yields $6.2 \times A_c$ according to Eq. (1). For this $A \gg A_c$ a cylinder-shaped deformation is predicted in [9] for which the Stoney approach is invalid.

4. Results

4.1. Compact wafers as calibration models

First, the FE results for the small thick (compact) wafer, i.e. the wafer with $D = 150$ mm and $h_s = 0.7$ mm, are examined to estimate the quality of our modelling approaches. With all used models (solids + shells, shells + shells, layered shells) the results are nearly identical with only tiny differences that can be explained by differences in discretization. Linear and nonlinear calculation schemes yield the same results, confirming that the problem may be solved sufficiently well within the small deformation theory. The values predicted by the extended Stoney approach are obtained in the Finite Element analyses, too. Both, the film stress and the deflection of the rim are identical within less than 1% deviation in most calculations. The worst FE result is obtained by the solid + shell combination where the deviation is 1.5% to the predicted values. For the wafer with isotropic substrate material, the film stress from the latter model is 949 MPa and the respective rim deflection is 0.04785 mm. Another important finding is that one contact algorithm, namely MPC–contact, in combination with the nonlinear geometry option yields in a huge error of about 50% deviation from the analytical prediction and from FE results with other models. We conclude that this contact option is useless for large deflection analyses.

As expected, there are large differences in calculation effort for the different modellings. The models using only shell elements yield comparable results independently of the element size. By contrast, the results of the models using the combination of solid and shell elements are size-dependent: models using solids with surface edge lengths similar to the wafer thickness, i.e. an aspect ratio approaching one, yield results comparable to the analytical predictions, whereas larger aspect ratios yield in increasing deviation from the predicted results with increasing aspect ratios.

If only nonlinear calculations with models using an average element edge length of 1 mm are considered, the effort of the different models can be compared: The model using a combination of solid plus shell elements with a contact algorithm needs about 17 h CPU time for the solution. About 1000 balance iterations, i.e. number of calls of the equation solver, are needed for this. Trying to use fewer, hence larger, time steps only increases the number of balance equations per time step, and thus, no accelerated solution is achieved. The models using only shell elements but contact for joining the layers are partly equally slow as the solid + shell-models. Only the pure shell models with common nodes, thus avoiding the contact formulations, converge significantly faster, i.e. with fewer balance equations even when fewer time steps are used. Then, the total CPU time decreases drastically to about 1 h and 30 min. This shows, that the use of a contact algorithm instead of using common nodes has a distinct effect of increasing the calculation time. This is because either additional balance equations are needed for the contact forces to be balanced (“pure penalty” method, “augmented Lagrange” method), or they introduce addition degrees of freedom (“normal Lagrange” algorithm), hence increase the size of the equation system. On the other hand, generating a mesh with common nodes requires equal meshes at the interfaces of both bodies. This is in the automatised mesh generation procedure of Ansys not provided. Using layered shells, however, does not need the generation of two layers of meshes because the layers are intrinsically embedded in every element. Beyond that, the layered shell elements show no benefit compared to the double layer of ordinary shell elements with common nodes, but also no disadvantages. The performance should be evaluated again for more layers.

We also examined the use of 4-node shell elements in comparison to 8-node shell elements. Using the higher approximation scheme of the 8-nodes elements, the result is only slightly better than from the 4-nodes elements: with the 8-node elements the rim deflection meets perfectly the theoretical value, whereas with the 4-node elements the rim deflection has a small deviation of 0.7%, i.e. 0.0532 instead of 0.0536 mm. In contrast, a benefit for using 4-nodes (shell) elements instead of 8-nodes elements, can not be detected: even with fewer nodes the calculation time does not decrease because more equilibrium iterations are needed.

A comparison between the true anisotropic substrate behaviour and the isotropic approximation exhibits no differences in the deflection of the small wafer.

4.2. Thin wafers

After verifying the capability of layered shell elements for modelling a coated wafer deformed by in-plane stresses, only layered shells are used for estimating the behaviour of thin large, i.e. slender, wafers. We use rather coarse meshes with element edge lengths between 1.3 and 2 mm to obtain “fast” results. The results of these element sizes are sufficiently converged towards a final solution as is shown in a masters thesis [14], where a thorough examination of the behaviour of thin wafers is done. Here, we give selected results. Even with these large elements, 10–35 thousand nodes are needed for the discretization of a quarter part of the double symmetric wafer. Because stability of the calculation is a serious challenge, about 800 time steps with a total of 1000–1500 equilibrium iterations are required to calculate the full temperature drop of 780 K. Thus, calculation time is some hours per run.

A second point to consider is the known bifurcation of the solution. After the bifurcation point a spherical solution exists but is not stable, i.e. a tiny imbalance suffices for a sudden twist of shape. In about one third of the runs, the shape change happened automatically, what sheds a light on the influence of tiny random imbalances in an otherwise deterministic procedure. In the other runs the shape change did not happen or happened delayed. Then, a pair of small counter-directional forces can be applied to enforce the shape change. If the forces are applied at the right moment they may be removed shortly after without a turn back to spherical, But if the forces are applied too early and then are removed, the

shape turns back into spherical. This behaviour can be used to determine the bifurcation point by simulation. The film stress at which the bifurcation happens can be compared to the prediction from Finot et al. [9], given by A_c and Eq. (1). It turns out, that the bifurcation point differs for the isotropic substrate in all simulations to that for anisotropic substrate behaviour, and for both from the predictions: We expected the shape change at about σ_c. All simulations with the isotropic substrate began loosing the spherical shape at a significant higher film stress, i.e. at about $1.25\,\sigma_c$. That is in concordance to what Masters and Salamon reported in [7]. The wafers with anisotropic substrate, however, began loosing their spherical shape earlier at about $0.9\,\sigma_c$.

Before transition to cylindrical deflection, the deflected shape of the wafer with the anisotropic substrate shows a distinct anisotropy: In [110]-direction the rim deflects less than in [100]-direction, see Fig. 1. The difference is about 4% of the absolute deflection, i.e. 13 μm at a deflection level of 0.31 mm. The wafer with isotropic substate behaviour, however, shows a perfect spherical shape, Fig. 2.

Using the equations in the appendix, the stresses and deflections according to the Stoney small deformations approach can be calculated for a particular temperature drop. That is: the wafer curvature, w'', from the thermal mismatch strain is found by Eq. (A.26) for a given ΔT, the film stress, σ^f, is then found by Eq. (A.20) using the calculated curvature, and finally, the warping is found by Eq. (A.27). The bifurcation and shape change are not predicted by this approach. The assumptions for this approach are a constant film stress on the wafer and the absence of in-plane shear stresses. As can be seen in Fig. 3, the first assumption of a constant film stress over the wafer area does not hold in the FE estimate. For the complete temperature drop of 780 °C the formulae predict a constant film stress on the anisotropic substrate of 1251 MPa. The FE result provides values between 1247 and 1258 MPa, depending on the location of the wafer, the higher values concentrated in the centre. But even though the film stress is not constant on the wafer area, the predicted value is met sufficiently well, i.e with less than 1% deviation from the prediction even for film stresses far above A_c correspondent to Eq. (1).

A different picture is obtained when the deflections are considered. For the wafer with anisotropic substrate behaviour, the prediction of the rim deflection at a film stress of 189 MPa, i.e. 94% of σ_c, is 0.532 mm. The FE result is 0.315 mm for this film stress, a deviation of over 40% from the prediction. For the wafer with isotropic substrate behaviour, the prediction is 0.477 mm for 193 MPa film stress, whereas the FE model yields a value of 0.289 mm, i.e. the prediction overestimates the FE result by 39%. At a film stress corresponding to $0.192\,\sigma_c$, i.e. 38.6 MPa, the prediction is 0.1085 mm for the anisotropic wafer and 0.0954 mm for the isotropic. The FE analyses yield in 0.1012 mm for the wafer with anisotropic substrate and 0.0901 mm for the isotropic. Here, the deviations from the predictions are only 6.7% and 5.6%, resp. A prediction for film stresses that lead to a cylindrical shape is not given by Stoney's approach, thus no comparison can be made. The absolute deflection at a film stress of 1251 MPa, turned out by FE analyses to be approximately 4.1 mm for the wafer with anisotropic and about 3.4 mm with isotropic substrate.

Finally, we consider the in-plane shear stresses $\sigma_{r\varphi}$ in the reference frame of the undeformed wafer. Fig. 4 shows these stresses in the thin film coating of a large thin wafer with anisotropic substrate at 189 MPa film stress. They are comparably small ranging between −0.011 MPa to +0.011 MPa but nevertheless they are not equal zero as assumed for the theoretical approach. For comparison, these stresses are less than ±0.00003 MPa in the film of the wafer with isotropic substrate. After the shape change, the shear stresses become even more pronounced, as depicted in Fig. 5. At a film stress of 1251 MPa they range between ±3.7 MPa and are also present in the isotropic wafer in similar size.

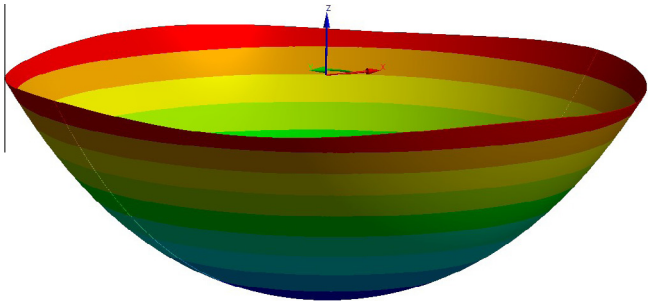

Fig. 1. Warping of a large thin wafer with anisotropic substrate material with a film stress of 189 MPa, i.e. at $0.94\,\sigma_c^f$. Displacements are scaled by factor 300. They range from 0 to 0.315 mm. The crystal axes are aligned with the shown coordinate system. Obvious is the larger warping in the crystal [100]-directions.

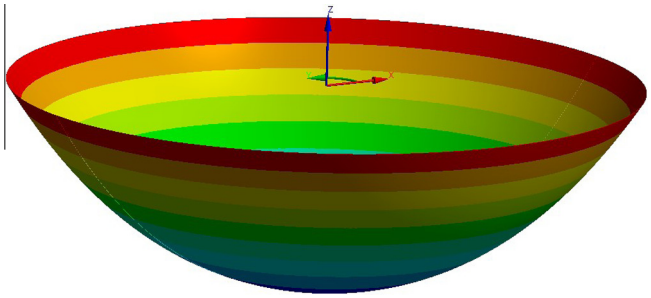

Fig. 2. Warping of a large thin wafer with isotropic substrate material with a film stress of 193 MPa. Displacements are scaled by factor 300. They range from 0 to 0.289 mm. Obvious is the perfect spherical warping.

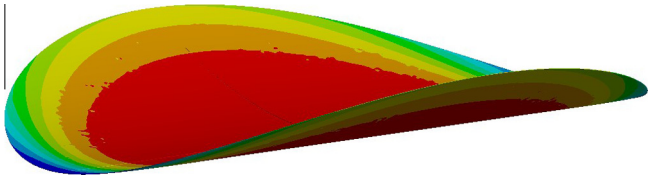

Fig. 3. Cylindrical warping of a large thin wafer at the highest film stress. Displacements are scaled by factor 10. They range from 0 to 4.1 mm. The colours depict the stress level (maximum principal stresses) from 1247 MPa (blue) at the flat part of the rim to 1258 MPa (red) in the centre. Obviously, the film stress decreases from centre to rim and along the rim from the bulged to the flat part. (For interpretation of the references to colour in this figure legend, the reader is referred to the web version of this article.)

5. Summary and conclusions

A wafer coated on one side with a metallic layer can be treated as a thin film on a substrate problem. An equation was derived by Stoney [1] to estimate the stress in a thin film on a bent strip of which the curvature is known. This equation is modified here for a circular anisotropic plate spherically bent by a thin coated film. An additional formula is derived by splitting the total strain into an elastic and a thermal part to estimate the curvature from the mismatch strain that originates from different thermal expansions of film and substrate. Thus, the warpage of the coated wafer can be estimated from the temperature change and the geometrical and material properties. Further, we used Finite Element analyses to estimate the bending behaviour of this warping problem numerically. The results from the FE models and the analytical approach were compared to each other.

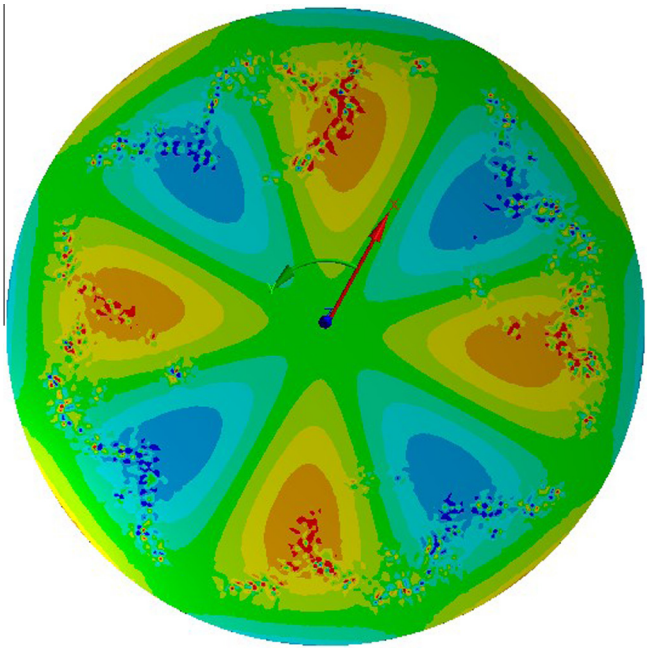

Fig. 4. In-plane shear stresses $\sigma_{r\varphi}$ in the film of a large thin wafer with anisotropic substrate behaviour at film stress 189 MPa. The colours depict the stress level ranging from −0.011 to +0.011 MPa. (For interpretation of the references to colour in this figure caption, the reader is referred to the web version of this article.)

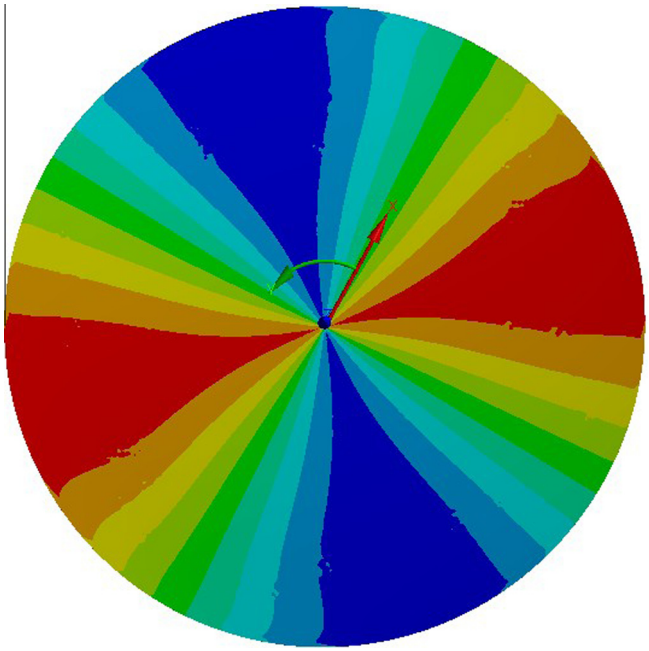

Fig. 5. In-plane shear stresses $\sigma_{r\varphi}$ in the film of a large thin wafer at the highest film stress of 1251 MPa. The colours depict the stress level ranging from −3.7 to +3.7 MPa. (For interpretation of the references to colour in this figure caption, the reader is referred to the web version of this article.)

The Finite Element analyses are divided into two parts. In a first step we calibrated the model used for FE analyses. For a comparably compact, i.e. small and thick, coated wafer the warping from thermal mismatch strains was calculated. It is shown that this problem can be treated in the framework of the small deformation theory. For comparison we used (a) combinations of solid elements for the substrate and shell elements for the film, connected either by common nodes or by contact algorithms, (b) arrangements of shell elements for substrate and film, and finally (c) a one layer model of layered shell elements, i.e. shell elements with an implicit layer formulation. The results from these analyses agree well with the results using the extended Stoney approach. Only the shell models with common nodes for joining turned out to be efficient enough for large thin wafers. Solid elements need an aspect ratio near one for good estimates. Therefore, the computational effort using solid elements increases disproportionately for very thin wafers. It could be verified that the usage of Ansys® "layered shell" elements is suitable for modelling this problem.

In a second step we calculated the warpage of a slender, i.e. large and thin, coated wafer using the latter element type and large deflection theory. The considered wafer has a diameter of 300 mm and is 0.2 mm thick. The coating film is about 1000 times thinner than the wafer. The considered film stress is of the size that leads to $6.2 \times A_c$ according to Finot et al. [9]. A distinct cylindrically shaped warpage can be obtained with this stress. Then, the out-of-plane deflection reaches 4.1 mm, i.e. about 20 times the wafer thickness. The point of bifurcation, i.e. the film stress at which a spherical curvature turns into a cylindrical shape, is different for substrate plates with an isotropic and anisotropic material behaviour, and for both it deviates from the prediction. The prediction given in [9] is a stress leading to A_c. The anisotropic substrate wafers turn into cylindrical shape at a film stress leading to $0.9A_c$, those with isotropic substrate at a film stress leading to about $1.25A_c$. For wafer with anisotropic substrate behaviour the FE simulation of the warping behaviour shows distinct anisotropic deflections prior to the shape change, whereas wafers with isotropic substrate behaviour deform perfectly spherical at this film stress level. Finally, the FE simulations exhibit that wafers with anisotropic substrates have distinct in-plane shear stresses $\sigma_{r\varphi}$ already during spherical warping and all wafers in the cylindrical shaped state.

Film stress estimates derived from the analytical procedure given in the appendix agree well with the results of FE calculations even for high stress levels that lead to multiples of the critical stress A_c. Curvature and subsequent deflection estimates by the analytical Stoney approach, however, agree well with FE results only when the stress–deflection relation is linear. For film stresses leading to $0.2A_c$ the deflection error becomes about 6%, for film stresses leading to A_c the error is about 40% compared to the FE results. For higher film stresses, the shape change is not predicted by this approach, and thus, the deflection can not be compared.

Acknowledgements

This work is performed in the project EPPL (Enhanced Power Pilot Line), co-funded by grants from Austria, Germany, France, Italy, Portugal and the Netherlands and the ENIAC Joint Undertaking. It is co-funded within the programme "Forschung, Innovation und Technologie für Informationstechnologie" by the Austrian Ministry for Transport, Innovation and Technology, bmvit.

Appendix A

Stoney's original formula considers a uniaxial strip bent by intrinsic stresses in a thin coating. Here, we derive it for a circular plate with a thin film stressed by thermal mismatch. We assume an uniform curvature $\kappa = 1/R$, where R is the deflection radius of the multibody plate. The thicknesses are h_s for the substrate and h_f for the film, $h_s \gg h_f$ and $h_f + h_s = H$. As far as possible we follow correspondingly the derivations of [15] and include the anisotropic extension found in [10].

We assume a cartesian coordinate system orientated along the crystal axes of the (0 0 1) silicon wafer. The x- and y-axes are in the neutral,i.e. the unstressed, wafer plane and the z-axis is perpendicular. w is the deflection in z-direction: $w = w(x) = u_z(x)$. It is also useful to define a ζ-coordinate in the z-direction but starting at the bottom of the wafer. The neutral plane is offset by α in z-direction and, thus, $z = \zeta - \alpha$.

The total strain is split into its elastic and thermal part $\varepsilon^{tot} = \varepsilon^{el} + \varepsilon^{\vartheta}$, of which only the elastic part contributes to stress, The thermal part of the film strain, $\varepsilon_f^{\vartheta}$, can be divided into the thermal part of the substrate, $\varepsilon_s^{\vartheta}$ and the discrepancy to that of the film, $\Delta\varepsilon_f^{\vartheta} = \Delta\alpha_f^{\vartheta}\,\Delta T = (\alpha_f^{\vartheta} - \alpha_s^{\vartheta})(T - T_0)$. α^{ϑ} is the thermal expansion coefficient and $T - T_0 = \Delta T$ the temperature increase or decrease from the starting temperature T_0 where the system is free of strains to the actual temperature T. The thermal expansion primarily elongates the body and only the misfit strain from the discrepancy of thermal expansion coefficients leads to warping. Hence, we assume that the curvature, Eq. (A.1), is due to the total strain minus the strain of the neutral plane. But the strain in the neutral plane is exactly the thermal strain. As the film is thin, the neutral plane is inside the substrate. With the total strain minus thermal strain equal elastic strain Eqs. (A.2) and (A.3) are valid for the substrate. For the film it must be corrected by adding the discrepancy thermal expansion between film and substrate, $\Delta\varepsilon_f^{\vartheta}$, Eq. (A.4).

From

$$\frac{1}{R} = \kappa = \frac{w''}{(1+w'^2)^{3/2}} \approx w''(x) = \frac{\partial^2 w}{\partial x^2} \tag{A.1}$$

and Bernoulli's assumptions for beam bending the elastic strains of the substrate can be expressed by

$$\varepsilon_{xx,s}^{el}(z) = -\frac{z}{R} \approx -z\frac{\partial^2 w}{\partial x^2} \tag{A.2}$$

$$\varepsilon_{yy,s}^{el}(z) = -\frac{z}{R} \approx -z\frac{\partial^2 w}{\partial y^2}, \tag{A.3}$$

for the film, it must be expressed by

$$\varepsilon_{xx,f}^{tot} - \varepsilon_s^{\vartheta} = \varepsilon_{xx,f}^{el}(z) + \varepsilon_f^{\vartheta} - \varepsilon_s^{\vartheta} = -\frac{z}{R} \approx -z\frac{\partial^2 w}{\partial x^2}. \tag{A.4}$$

Hooke's law for plane stress, i.e. $\sigma_{zz} = 0$, in the more general case of cubic anisotropic materials, reads

$$\sigma_{xx} = q_{11}\varepsilon_{xx}^{el} + q_{12}\varepsilon_{yy}^{el} \tag{A.5}$$

$$\sigma_{yy} = q_{12}\varepsilon_{xx}^{el} + q_{11}\varepsilon_{yy}^{el} \tag{A.6}$$

$$\sigma_{xy} = c_{33}\gamma_{xy}^{el} \tag{A.7}$$

with

$$q_{11} = c_{11} - \frac{c_{12}^2}{c_{11}} \tag{A.8}$$

$$q_{12} = c_{12} - \frac{c_{12}^2}{c_{11}} \tag{A.9}$$

and c_{ij} being the constants of the cubic anisotropic elasticity matrix c_{11}, c_{12}, c_{33}. If the curvatures are equal in x- and y-directions,

$$\frac{\partial^2 w}{\partial x^2} = \frac{\partial^2 w}{\partial y^2} = w'' \tag{A.10}$$

then it follows for the substrate with Eq. (A.2) in (A.5) using Eq. (A.10)

$$\sigma_{xx}^s = \sigma_{yy}^s = (q_{11} + q_{12})(-zw''). \tag{A.11}$$

With the transformation rule

$$\sigma_{rr} = \cos^2\varphi\;\sigma_{xx} + \sin^2\varphi\;\sigma_{yy} + \sin 2\varphi\;\sigma_{xy} \tag{A.12}$$

and neglecting shear stresses, i.e. $\sigma_{xy} = 0$, if follows $\sigma_{rr} = \sigma_{xx}$ and Eq. (A.11) becomes

$$\sigma_{rr}^s = -E^* z w'' \tag{A.13}$$

with

$$E^* = q_{11} + q_{12} = c_{11} + c_{12} - 2\frac{c_{12}^2}{c_{11}} \tag{A.14}$$

$$= \frac{E}{1-\nu} \quad \text{(for isotropic materials)}$$

E and ν are Young's modulus and Poisson's ratio, resp.

After these preliminaries, we consider the stresses in the wafer at any point, assuming constant curvature w'' everywhere in the wafer. Since there are no external loadings, the system must be in equilibrium at every point, thus the sums of forces and of moments must be 0:

$$\int_0^H \sigma_{rr}(z)\,d\zeta = \int_0^{h_s} \sigma_{rr}^s(z)\,d\zeta + \int_{h_s}^H \sigma_{rr}^f\,d\zeta = 0 \tag{A.15}$$

$$\int_0^H \sigma_{rr}(z) z\,d\zeta = \int_0^{h_s} \sigma_{rr}^s(z) z\,d\zeta + \int_{h_s}^H \sigma_{rr}^f z\,d\zeta = 0 \tag{A.16}$$

Using $z = \zeta - \alpha$ and assuming constant film stress over the film thickness due to its tiny height, Eqs. (A.15) and (A.16) become

$$E_s^*\left(\frac{\zeta^2}{2} - \alpha\zeta\right)w''\Big|_0^{h_s} = E_s^* w'' h_s\left(\frac{h_s}{2} - \alpha\right) = \sigma_{rr}^f h_f \tag{A.17}$$

and

$$0 = -E_s^* w'' \int_0^{h_s} (\zeta - \alpha)^2\,d\zeta + \sigma_{rr}^f \int_{hs}^H (\zeta - \alpha)\,d\zeta$$

hence

$$E_s^* w'' \frac{h_s}{3}\left(h_s^2 - 3h_s\alpha + 3\alpha^2\right) = \sigma_{rr}^f h_f\left(\frac{h_f}{2} + h_s - \alpha\right) \tag{A.18}$$

From Eqs. (A.17) and (A.18) the ζ-coordinate α of the neutral plane becomes

$$\alpha = \frac{(2h_s + 3h_f)h_s}{6(h_s + h_f)} \tag{A.19}$$

that is for negligible film thicknesses, $h_f \to 0, \alpha = h_s/3$. With α dissolved, σ_{rr}^f from Eq. (A.17) can be rewritten:

$$\sigma_{rr}^f = \frac{h_s^3}{6h_f(h_s + h_f)} E_s^* w'' \tag{A.20}$$

With $h_f + h_s \to h_s$, Eq. (A.20) is the Stoney formula [1] modified for plates:

$$\sigma_{xx}^f h_f = \frac{1}{6} E_s^* \frac{h_s^2}{R}. \tag{A.21}$$

To calculate the curvature as a result of the thermal mismatch strain, we consider that the film adheres to the substrate and there may be no (horizontal) gap. Hence, the total strains at the interface must be equal:

$$\varepsilon_s^{tot}(\zeta = h_s) = \varepsilon_f^{tot}(\zeta = h_s) \tag{A.22}$$

Hence,

$$\varepsilon_s^{tot}(\zeta = h_s) = \varepsilon_s^{el}(\zeta = h_s) + \varepsilon_s^{\vartheta} = -(h_s - \alpha)w'' + \varepsilon_s^{\vartheta} \tag{A.23}$$

and

$$\varepsilon_f^{tot}(\zeta = h_s) = \frac{\sigma_{rr}^f}{E_f^*} + \varepsilon_s^{\vartheta} + \Delta\varepsilon_f^{\vartheta} \tag{A.24}$$

it follows

$$-(h_s - \alpha)w'' = \frac{\sigma_{rr}^f}{E_f^*} + \Delta\varepsilon_f^{\vartheta} \tag{A.25}$$

and finally, with α from Eq. (A.19) and σ_{rr}^{f} from Eq. (A.20) it follows:

$$w'' = -\Delta\alpha_f^{\vartheta}\Delta T \frac{6h_f E_f^*(h_s + h_f)}{E_s^* h_s^3 + h_s h_f E_f^*(4h_s + 3h_f)} \tag{A.26}$$

With the given curvature w'' the film stress σ_{rr}^{f} can be calculated using Eq. (A.20).

For w'' being a constant in this case and uniform across the wafer, integrating twice with respect to x leads to the deflection

$$w(x) = \frac{1}{2}w''x^2 + C_1 x + C_2 \tag{A.27}$$

with the two integration constants $C_1 = C_2 = 0$, since $w(x = 0) = 0$, and, from symmetry contition at $y = 0, w'(x = 0) = 0$.

References

[1] Stoney GG. The tension of metallic films deposited by electrolysis. Proc R Soc London A 1909;82:172–5.

[2] Draney NR, Liu JJ, Jiang T. Experimental investigation of bare silicon wafer warp. In: IEEE Workshop on microelectronics and electron devices; 2004. p. 120–3.

[3] Chen J, De Wolf I. Study of damage and stress induced by backgrinding in Si wafers. Semicond Sci Technol 2003;18:261–8.

[4] Jinglong S, Fei Q, Chao R, Zhongkang W, Liang T. Residual stress measurement of the ground wafer by raman spectroscopy. In: Electronic packaging technology (ICEPT), 2014 15th international conference on; 2014. p. 867–70.

[5] Harper BD, Wu C-P. A geometrically nonlinear model for predicting the intrinsic film stress by the bending-plate method. Int J Solids Struct 1990;26 (5–6):511–25.

[6] Masters CB, Salamon NJ. Geometrically nonlinear stress–deflection relations for thin film/substrate systems. Int J Eng Sci 1993;31(6):915–25.

[7] Masters CB, Salamon NJ. Geometrically nonlinear stress–deflection relations for thin film/substrate systems with a finite element comparison. J Appl Mech 1994;61:872–8.

[8] Salamon NJ, Masters CB. Bifurcation in isotropic thin film/substrate plates. Int J Solids Struct 1995;32(3/4):473–81.

[9] Finot M, Blech IA, Suresh S, Fujimoto H. Large deformation and geometric instability of substrates with thin-film deposits. J Appl Phys 1997;81:3457.

[10] Janssen CGAM, Pujada BR. Elastic deformation of silicon (001) wafers due to thin film stresses. Appl Phys Lett 2007;91:121913.

[11] Janssen CGAM, Abdalla MM, van Keulen F, Pujada BR, van Venrooy B. Celebrating the 100th anniversary of the stoney equation for film stress: developments from polycrystalline steel strips to single crystal silicon wafers. Thin Solid Films 2009;517(6):1858–67.

[12] Schicker J, Arnold T, Hirschl C, Iravani A, Kraft M. Simulation of the deformation behaviour of large thin silicon wafers and comparison with experimental findings. In: Thermal, mechanical and multi-physics simulation and experiments in microelectronics and microsystems (EuroSimE), 2015 16th International Conference on; 2015. p. 1–6.

[13] Hopcroft MA, Nix WD, Kenny TW. What is the young's modulus of silicon? J Microelectromech Syst 2010;19:229–35.

[14] Khan WA. FEM simulation of the thermo mechanical behaviour of Si-metal composites [Master's thesis]. CTR AG Villach and University Duisburg-Essen (in preparation).

[15] Schwarzer N. About the theory of thin coated plates, published online at <http://nbn-resolving.de/urn:nbn:de:bsz:ch1-200200050>, TU Chemnitz (Jan. 2002)